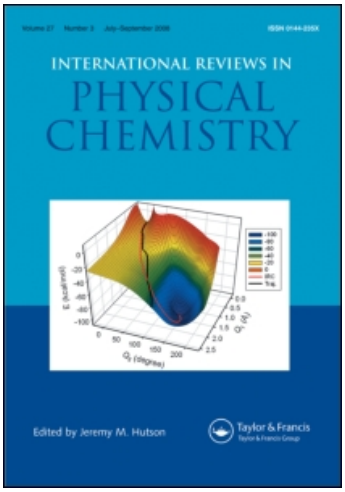

International Reviews in Physical Chemistry
Publication details, including instructions for authors and subscription information:
http://www.informaworld.com/smpp/title~content=t713724383

Optically-heterodyne-detected optical Kerr effect (OHD-OKE): Applications in condensed phase dynamics

Neil A. Smith; Stephen R. Meech

Online publication date: 26 November 2010

To cite this Article Smith, Neil A. and Meech, Stephen R.(2002) 'Optically-heterodyne-detected optical Kerr effect (OHD-OKE): Applications in condensed phase dynamics', International Reviews in Physical Chemistry, 21: 1, 75 — 100
To link to this Article: DOI: 10.1080/01442350110092701
URL: http://dx.doi.org/10.1080/01442350110092701

INT. REVIEWS IN PHYSICAL CHEMISTRY, 2002
VOL. 21, NO. 1, 75–100

Taylor & Francis
Taylor & Francis Group

Optically-heterodyne-detected optical Kerr effect (OHD-OKE): applications in condensed phase dynamics

NEIL A. SMITH and STEPHEN R. MEECH†
School of Chemical Sciences, University of East Anglia, Norwich NR4 7TJ, UK

The ultrafast optically-heterodyne-detected optical Kerr effect (OHD-OKE) is established as a relatively simple tool for recording the ultrafast dynamics of liquids with high temporal resolution and excellent signal-to-noise ratios. The principles and practice of the OHD-OKE method are outlined. Its application in recording the dynamics of several molecular liquids is described. The data are discussed in terms of the underlying microscopic molecular motions. Orientational motion—both librational and diffusive—is responsible for a significant fraction of the dynamics. Other potential contributions are discussed, but these are less readily assigned. The application of OHD-OKE measurements in interpreting ultrafast studies of the optical dynamics of solutions is discussed. Finally the extension of OHD-OKE methods to record the dynamics of more complex, heterogeneous, media is described.

Contents

1. Introduction

The subject of this review, the ultrafast optically-heterodyne-detected optical Kerr effect (whose acronym, OHD-OKE, is hardly less of a mouthful) must be regarded as a relative youngster compared with the electro-optic Kerr effect (1875 [1]) or even the optical Kerr effect (predicted 1956 [2], observed 1964 [3, 4]).

† Email: s.meech@uea.ac.uk

International Reviews in Physical Chemistry ISSN 0144–235X print/ISSN 1366–591X online © 2002 Taylor & Francis Ltd
http://www.tandf.co.uk/journals
DOI: 10.1080/01442350110092701

However, within the realm of ultrafast spectroscopy, OHD-OKE is one of the longest established and most widely applied methods of capturing the ultrafast dynamics of a sample. There are at least three reasons for its popularity. First, the implementation of the experiment is relatively straightforward, by the standards of ultrafast spectroscopy. Second, the experiment provides data of extremely high signal-to-noise ratio, permitting detailed analysis. Third, as a result of the high signal-to-noise ratio, deconvolution procedures are possible, which yield a time resolution in the experiment which is greatly superior to the temporal pulse width of the laser employed. Recently these favourable characteristics have lead to the OHD-OKE method being applied in an extremely wide range of problems in condensed phase dynamics. In the following we shall present an overview of the OHD-OKE method and describe its application to several condensed-phase systems.

The origin of the OKE signal is simply described in the following way. A linearly polarized optical pulse interacting with an initially isotropic sample will induce a transient birefringence. A second, time-delayed, pulse, incident at the same point in the sample, with its plane of polarization oriented at some angle to that of the first, will experience a birefringent medium, and will thus emerge from the sample elliptically polarized [5]. A polarizer, crossed with the plane of polarization of the second pulse, is placed in front of a detector. The birefringence induced in the sample causes a fraction of the second pulse to reach the detector. This is the OKE signal. In a time-resolved OKE experiment the signal is monitored as a function of delay time between the first and second pulses, and the relaxation of the birefringence induced in the sample is measured. In an ultrafast OKE experiment very short pulses are employed, which implies a large spectral width, typically several hundred wavenumbers. In molecular liquids the sample polarizability will exhibit resonances, owing to rotational and vibrational motion. If these resonances arise from Raman-active modes, and they lie within the bandwidth of the laser, they may be coherently excited, as shown in figure 1. Excitation of these modes contributes to the OKE signal, and the frequency of the mode can be detected in the time-resolved

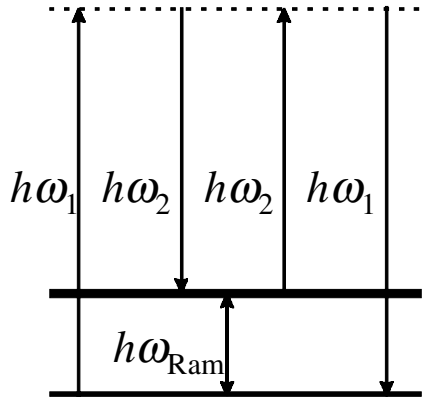

Figure 1. An energy level diagram for the OKE. The diagram illustrates the excitation of Raman active modes in the experiment. In the ultrafast measurement both frequencies ω_1 and ω_2 are contained in the spectrally broad pulse, which typically limits the observable modes to $\omega_{\mathrm{Ram}}/c < 500\,\mathrm{cm}^{-1}$. Note that the diagram is not intended to denote the time orderings in the measurement. (For a more sophisticated diagrammatic approach see [6].)

measurement. When the two frequencies arise from two different laser sources this is called the Raman-induced Kerr effect (RIKE) [7], and OHD-RIKES and OHD-OKE are used more or less interchangeably when spectrally broad pulses are employed.

The measurement, origin and detection of the OHD-OKE signal are described in more detail in the next section. Applications of the experiment are reviewed in section 3, focusing initially on the dynamics of pure liquids, but considering also liquid mixtures and heterogeneous media. The review ends with a summary.

2. Measurement

2.1. *Origin and detection of the OHD-OKE signal*

The apparatus for the OHD-OKE measurement is shown in figure 2 and is used with little variation in many laboratories. The source of the ultrafast pulses is, almost invariably, a self-mode-locked titanium sapphire laser. The availability of these stable robust solid-state sources, which routinely produce near-transform-limited sub 50 fs pulses, has greatly expanded the capabilities of ultrafast laser laboratories. For many resonant optical experiments the near-infrared (IR) frequencies generated are not useful, which has stimulated much recent progress in the development of optical parametric amplifiers [8, 9]. However, for non-resonant experiments, such as OHD-OKE, IR frequencies are nearly ideal, being in most cases far removed even from two-photon electronic resonances.

The remainder of the apparatus may be constructed from commonly available optical components (figure 2). The output of the Ti : sapphire laser passes through a prism pair compressor to compensate for pulse broadening group velocity dispersion (GVD) in the laser, and also for pre-compensation, to correct for GVD in the subsequent optical path [10]. The beam from the compressor is routed to a beam splitter, which reflects about 1% of the intensity. The transmitted beam, the 'pump', passes through a mechanical chopper, a half-wave plate and a polarizer, and is focused onto the sample. The reflected beam, the 'probe', passes through a second 1% beamsplitter (which yields a signal for monitoring and correcting for laser

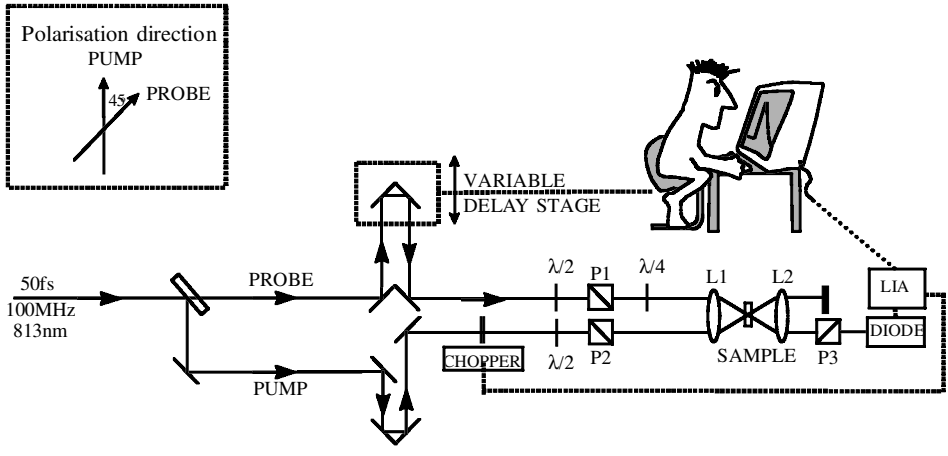

Figure 2. Schematic of a typical layout for the ultrafast OHD-OKE experiment. See text for details.

intensity variation, if required) and is routed to a back-reflecting mirror pair mounted on a motorized translation stage, which has submicron positional accuracy and reproducibility. This delay stage controls the pump–probe delay time. The probe beam then passes a half-wave plate, a polarizer and a quarter-wave plate before being focused onto the sample. The pump and probe beams cross at a small angle in the sample. The sample, be it liquid, solid or heterogeneous, should be of high optical quality, since scattered pump radiation can seriously degrade signal to noise in the final OHD-OKE trace. For example, liquids should usually be carefully filtered to remove scattering particles. The transmitted pump radiation is sent to a beam dump, while the transmitted probe radiation is recollimated, routed through a second polarizer and detected by a photomultiplier or amplified photodiode. The output of the detector is measured by a lock-in amplifier which is referenced to the frequency of the chopper in the pump beam. The modulated signal intensity is recorded by a computer which also controls the pump–probe delay. In some cases both pump and probe beams are modulated and the lock-in is referenced to the sum or difference frequency [11]. This goes some way towards minimizing the scattered light signal mentioned above. Further attenuation in scattered light can be achieved by spatial filtering and/or placing the detector behind a pinhole some distance from the sample. However, in general it is preferable first to minimize spurious scattered light by careful sample preparation.

If scatter can be suppressed the quality of OHD-OKE data is to a large degree determined by the quality of the polarization control. All waveplates should be of the broadband type, to apply phase delay uniformly to all frequencies in the spectrally broad laser pulse. The first polarizers in the pump (P_1) and probe (P_2) beams are of the same type, so that pump and probe beams pass equal amounts of glass, and so acquire equivalent GVD (hence also the need for the second beamsplitter in the probe beam, since in our experience correction for intensity variation of the laser source is seldom necessary). The GVD in the optical path may then be pre-compensated by adjusting the prism pair separation while monitoring the background-free second-harmonic autocorrelation trace, which is measured in a thin nonlinear crystal located at the sample position [12]. This autocorrelation trace, $G^{(2)}(t)$, is an important parameter in the subsequent analysis of the data. In general it is not sufficient simply to minimize the pulsewidth. The spectrum must also be measured to check that the pulses employed in the analysis (see below) are as close as possible to the transform limit [12]. In the most commonly employed OHD-OKE geometry the polarizer P_1 and waveplate in the pump beam are set to pass linearly polarized light. The probe polarization is rotated an angle of 45° and the polarizer P_2 is set at this angle. The fast axis of the quarter-wave plate is also initially aligned with the probe polarization direction. In the absence of the pump pulse the polarizer P_3 is crossed with P_2 to achieve maximum extinction. There will inevitably be strain birefringence in the focusing lenses and the sample. This can be corrected for by iteratively adjusting the angle of the quarter-wave plate and P_3 to maximize extinction [13]. This procedure ensures linear polarization of the probe in the sample. Finally the extinction after P_3 should be better than 5×10^{-6}, which requires polarizers of good quality. Anything less will degrade the quality of the data.

Detailed theoretical treatments of the signal detected behind P_3 have been given by several groups. An early and still helpful discussion was given by Sala and Richardson [14]. Cho *et al.* presented a rather complete theory of off-resonant transient birefringence, using the density matrix approach [15]. Kinoshita *et al.*

described the origin of the OHD-OKE signal with careful attention to the polarization [16]. Here we will follow their development (in an abbreviated form) as it highlights the importance of polarization control.

The oscillating electric field of the pump pulse, taken to be polarized in the x direction, induces an index anisotropy in the sample. The probe pulse propagates along the z axis with a linear polarization an angle ϕ from the pump polarization. The analysing polarizer P_3 is oriented at an angle ψ. The electric field of the probe pulse after the sample is expressed as

$$E_{\mathrm{p}}^{*}(t) = E_{\mathrm{p}}(t)\exp\left[\mathrm{i}\omega\left(\frac{n_0 z}{c} - t\right)\right]\left(1 + \frac{\mathrm{i}\omega n_2 z}{c} + \cdots\right), \tag{1}$$

in which $E_{\mathrm{p}}(t)$ is the incident electric field, n_0 the refractive index in the absence of the pump field and n_2 the lowest non-zero term in the nonlinear index of refraction:

$$n_2 = \int_{-\infty}^{t} \mathrm{d}t'\, R(t - t')I(t'). \tag{2}$$

In equation (2) $R(t)$ is the material response function, related to the time differential of the third-order susceptibility, a fourth-rank tensor, and $I(t)$ is the temporal profile of the pump pulse. In an isotropic and transparent medium the only independent tensor elements contributing to the response function are R_{xxxx} and R_{yyxx} [7] so the electric field of the components of the probe pulse (1) in the direction ψ are expressed as [16]

$$\begin{aligned} E_{\mathrm{p}\psi} = \cos\psi\Bigg\{ & E_{\mathrm{p}x}(t-\tau)\exp\left[\mathrm{i}\omega\left(\frac{n_0 z}{c} - t + \tau\right)\right] \\ & \times\left[1 + \mathrm{i}\,\frac{wz}{c}\int_{-\infty}^{t}\mathrm{d}t'\, R_{xxxx}(t-t')E_{\mathrm{e}}(t')E_{\mathrm{e}}(t')\right]\Bigg\} \\ & + \sin\psi\Bigg\{ E_{\mathrm{p}y}(t-\tau)\exp\left[\mathrm{i}\omega\left(\frac{n_0 z}{c} - t + \tau\right)\right] \\ & \times\left[1 + \mathrm{i}\frac{wz}{c}\int_{-\infty}^{t}\mathrm{d}t'\, R_{yyxx}(t-t')E_{\mathrm{e}}(t')E_{\mathrm{e}}(t')\right]\Bigg\}, \end{aligned} \tag{3}$$

in which τ is the pump–probe delay time. If the polarizers P_1 and P_2 are left crossed the relatively weak homodyne signal is detected. However, if P_2 is rotated by an angle θ the components of the electric field of the probe beam are

$$E_{\mathrm{p}x} = E_{\mathrm{p}}(\cos\theta\cos\phi - \mathrm{i}\sin\theta\sin\phi) \tag{4}$$

and

$$E_{\mathrm{p}y} = E_{\mathrm{p}}(\cos\theta\sin\phi + \mathrm{i}\sin\theta\cos\phi). \tag{5}$$

The effect of the rotation of P_2 is to introduce a local oscillator, a fraction of the probe field, temporally and spatially overlapped with the signal. On substituting equations (4) and (5) into equation (3) and assuming a square-law detector the observed light intensity is obtained from $I(\tau) = \langle E_{\psi}E_{\psi}^{*}\rangle_t$ where the angle brackets mean a statistical average over the pump and probe electric fields, and temporal integration due to the response time of the detector. Performing this operation, taking θ as small, and assuming the conventional OHD-OKE geometry ($\phi = -\psi = 45^{\circ}$) yields

$$I(\tau) = \langle I_p \sin^2\theta \rangle_t + \left\langle \left| E_p(t-\tau)\frac{\omega z}{c}\int_{-\infty}^{t} dt'\, R_a(t-t')I(t') \right|^2 \right\rangle_t + 2\left\langle I_p(t-\tau)\frac{\omega z}{c}\sin\theta \int_{-\infty}^{t} dt'\, R_a(t-t')I(t') \right\rangle_t, \quad (6)$$

in which $R_a(t) \equiv R_{xxxx}\cos\phi\cos\psi + R_{yyxx}\sin\phi\sin\psi$. Thus the signal contains three contributions. The first term is simply the transmitted probe intensity, which will be unmodulated, so it is not detected by the lock-in amplifier. From an experimental point of view it should not be neglected, as its intensity may be high, and can lead to saturation of the detector. This is of course easily avoided by appropriate attenuation. In addition this large signal occupies an appreciable portion of the dynamic range of the lock-in amplifier. Fourkas and coworkers developed a subtraction scheme to overcome this problem, thus attaining excellent dynamic range in their measurements [17]. The second term is the homodyne contribution to the signal, which is present even when $\theta = 0°$. The third term is the heterodyne contribution, the OHD-OKE signal of principal interest. It will usually be the dominant term when θ is only 1°. The advantages of heterodyne detection are clear from equation (6). First, the signal is linear in the response function, which implies improved signal to noise and means that the same dynamics relaxes more slowly in heterodyne than in homodyne ($\propto R_a^2$) detection. Second, the signal depends linearly on pump intensity, again improving signal to noise. Finally the signal can be made larger by increasing θ (but see above).

Since both the second and third terms of equation (6) are detected by the lock-in amplifier, and they relax with different rates, it is desirable to have a means of separating them. If measurements are made at $\pm\theta$ the third term changes sign, while the second does not. Thus the pure heterodyne signal is recovered from the difference of the two measurements, while the pure homodyne response can be extracted from their sum [18]. In practice when θ is in the range 0.5°–1.5° the homodyne signal is very small relative to the heterodyne signal. An example of the quality of the data available from the heterodyned signal is shown in figure 3.

Finally it is worth emphasizing that rotating analyser P_2 yields an out-of-phase local oscillator, which probes the pump-induced birefringence, as required for OHD-OKE. Rotation of P_3 introduces an in-phase local oscillator, which entails a different measurement, the sample dichroism [18–20]. This signal, which has been discussed in detail by Waldeck and coworkers, is extremely useful when the laser frequency is resonant with an electronic transition [19, 20]. This experiment, generally labelled ultrafast polarization spectroscopy, reveals the excited and ground state population and reorientation dynamics of the resonant solute. It will not, however, be discussed further here, where the focus is on off-resonance measurements. It also is worth noting that the generation of a local oscillator by rotation of the quarter-wave plate, or through the existence of strain birefringence in the sample, yields a mixture of dichroism and birefringence that is not readily analysed.

2.2. *Analysis of the OHD-OKE signal*

The third (heterodyne) term of equation (6) will usually be the dominant contribution to the signal, and it may be rigorously isolated in the manner described above. If the pump and probe pulses originate from the same laser source the signal

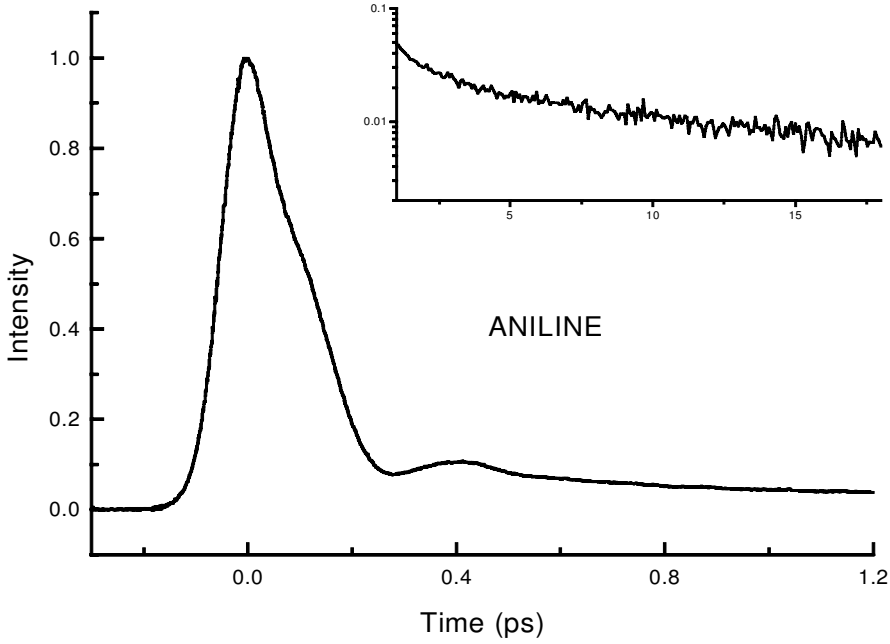

Figure 3. The OHD-OKE signal from liquid aniline, showing the excellent quality of the data available from the method. Note the appearance of an instantaneous response which follows the excitation pulse (autocorrelation width 72 fs), a rapid oscillation, damped on a subpicosecond timescale, and a biexponential picosecond relaxation (inset).

can be expressed as a convolution of the background-free second-harmonic autocorrelation trace $G^{(2)}(t)$, with the material response function $R_a(t)$

$$I(\tau) \propto \int \mathrm{d}t\, R_a(t-\tau) G^{(2)}(t). \tag{7}$$

The analysis of equation (7) was developed in a series of papers by McMorrow, Lotshaw and their coworkers [18, 21–27]. Both $I(\tau)$ and $G^{(2)}(t)$ are available with high signal to noise, the latter invariably being measured at the sample position and with an identical geometry to $I(\tau)$, which is important to ensure that $t = 0$ is accurately determined [18]. The sample response $R_a(t)$ can then be recovered from the convolution (7) through the following Fourier transform relationship:

$$F[R_a(t)] = \frac{F[I(\tau)]}{F[G^{(2)}(\tau)]} = D(\omega), \tag{8}$$

in which F indicates a forward complex Fourier transform. Thus the sample dynamics can be recovered, in the frequency domain, $D(\omega)$, undistorted by convolution with the finite pulsewidth of the laser [23]. The sample response contains contributions from both the nuclear dynamics, $r(t)$, of principal interest here, and the instantaneous electronic response, $\sigma(t)$, arising from the electronic part of the nonlinear susceptibility,

$$R_a(t) = \sigma(t) + r(t). \tag{9}$$

Since the electronic component is real it will not contribute to the imaginary part of $D(\omega)$, $\mathrm{Im}[D(\omega)]$, and then the nuclear dynamics can be recovered from the inverse transform

$$r(t) = 2F^{-1}\{\mathrm{Im}[D(\omega)]\}\Phi(t - t_0) \tag{10}$$

in which $\Phi(t)$ is the Heaviside step function and F^{-1} represents an inverse Fourier transform. Thus the nuclear dynamics is recovered in the time domain. Of course the frequency domain representation, $\mathrm{Im}[D(\omega)]$, contains identical information and is often employed in subsequent analysis, as it is directly comparable with data obtained in dynamic light scattering (DLS) experiments; $\mathrm{Im}[D(\omega)]$ is often referred to as the Raman spectral density. Considerable efforts have been made to establish that this spectral density is identical to that extracted from DLS measurements [28, 29]. Indeed, the same spectral density may be extracted from several different off-resonance optical experiments, and Friedman and She have presented a useful table showing the connections between these [30]. Although the light scattering and OHD-OKE spectral densities are completely equivalent there are some distinct advantages in extracting the data from time domain measurements: high resolution may be obtained by collecting (or simulating—see below) a large number of data points; the data are undistorted by the thermal Bose–Einstein occupation factor, so the manipulations commonly employed in DLS experiments [31] to extract the lowest-frequency components of the spectral density are not required; the unwanted contributions of scattered light are more readily removed from time domain data.

The electronic response is not redundant, as it can be used to gain information on the electronic hyperpolarizability, a parameter of practical importance in the characterization of nonlinear optical materials. A relative value for σ can be obtained from the magnitude of the amplitude in the time domain at $t = 0$ [32] or from the constant value found in the real part of $D(\omega)$ [23, 33].

In figure 3 the OHD-OKE data for liquid aniline were shown. In figure 4 the recovered $\mathrm{Im}[D(\omega)]$ is presented. It is clear that the time domain data reveal liquid dynamics on a wide range of timescales, subpicosecond to tens of picoseconds. Such a range of timescales introduces a potential problem into the determination of $\mathrm{Im}[D(\omega)]$. To obtain the high resolution seen in figure 4 it is necessary to have (a) an accurately determined time zero and (b) data obtained with high time resolution. Both suggest step sizes of about 1 fs. It would clearly be tedious to record the 10^5 data points required to cover adequately both the slow and fast dynamics observed. Fortunately the oscillatory behaviour seen in figure 3 usually dies out in a few picoseconds, and the response on the picosecond timescale is well represented by a biexponential function. Hence it is adequate to perform high-time-resolution measurements over a few picoseconds and much coarser resolution measurements over the time of the slow exponential dynamics. The latter can then be fitted to recover the exponential time constants and their relative weights. These data can then be used to extend artificially the high-time-resolution measurement with the same 1 fs step size [18]. The result of one such Fourier transform analysis (8) is shown in figure 4. Alternatively, since it is often the ultrafast dynamics which are of interest, the exponential tail can be subtracted from the high-time-resolution data, and the resultant data file extended with zeros (so-called 'zero padding') [23, 25]. In this case the ultrafast (or reduced) spectral density is recovered, $\mathrm{Im}[(D'(\omega)]$. The ultrafast spectral density of liquid aniline is shown in figure 5. In either case a well-resolved

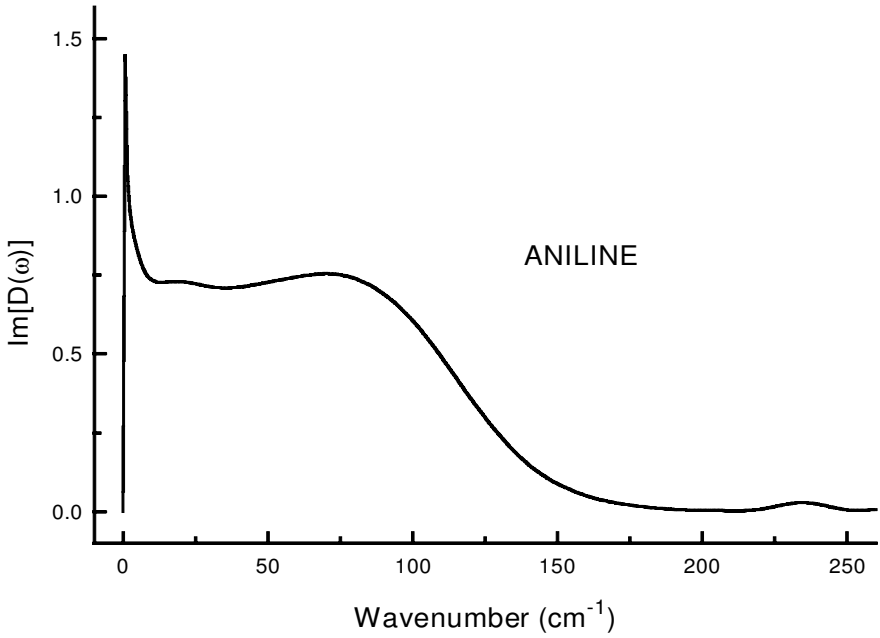

Figure 4. The spectral density, Im[$D(\omega)$], for liquid aniline, recovered from the data of figure 3 and the measured $G^{(2)}(t)$ in the manner described in the text.

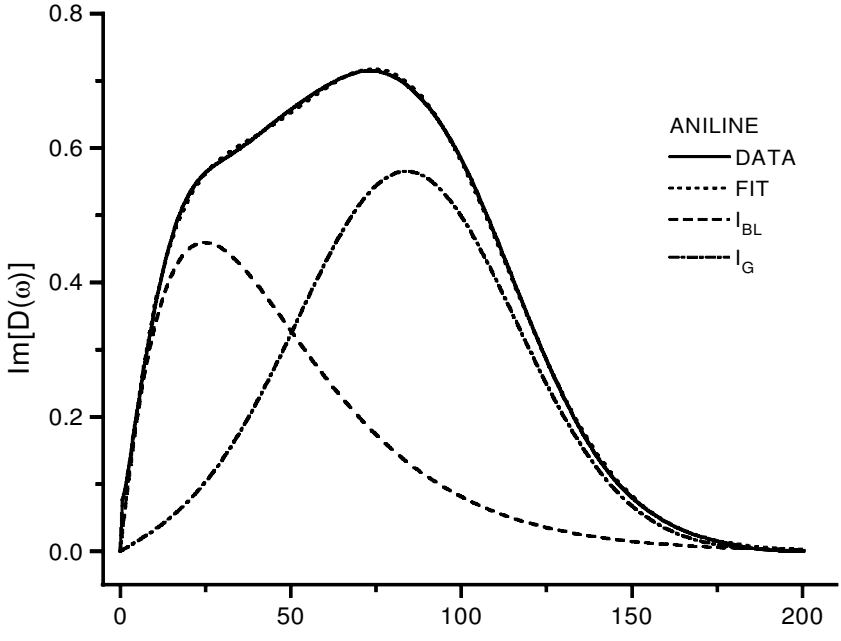

Figure 5. The ultrafast spectral density, Im[$D'(\omega)$], for liquid aniline fit to equations (18) + (19). Both the quality of fit and the contributions of the individual components are shown.

spectral density with high signal to noise is obtained, often over a range of several hundred wavenumbers. This is ideal for subsequent analysis.

3. Applications

3.1. *Dynamics of pure liquids*

Many of the earliest OHD-OKE measurements focused on understanding the ultrafast dynamics of pure liquids and this continues to be a major objective [11, 13, 21–27, 32–56]. These studies complement the extensive literature on DLS studies of liquid-state dynamics [57–59]. The potential advantages of the OHD-OKE method over DLS were outlined above. However, in either case the objective is to connect the macroscopic measurement of the sample dynamics, $r(t)$ or $\mathrm{Im}[D(\omega)]$, to the microscopic, molecular dynamics of the liquid. The foundations of this connection will only be outlined very briefly here, as they have been described by several groups [57–63], the development followed below being given in more detail by Ladanyi and coworkers [61, 62].

In the classical high-temperature limit the sample response function, $r(t)$, is related to the time derivative of the time correlation function of the anisotropic component of the collective system polarizability, Π_{xz} [62–64]

$$r(t) = -\frac{1}{kT}\Phi(t)\frac{\partial}{\partial t}\Psi_{xz}(t) \tag{11}$$

where

$$\Psi_{xz}(t) = \frac{\langle \Pi_{xz}(0)\Pi_{xz}(t)\rangle}{\frac{1}{15}N\gamma^2} \tag{12}$$

in which N is the number density of molecules and γ^2 is the square of the molecular polarizability anisotropy of the isolated molecule. (Essentially the same time correlation function appears with different designations, including $C_2(t)$, $C_\Pi(t)$ and $C_{\mathrm{Ray}}(t)$, where the subscript in each case indicates a polarizability measurement.) In the liquid phase the collective system polarizability Π is the sum of all single-molecule polarizabilities α and the 'interaction-induced' components, which arise from intermolecularly induced dipole interactions:

$$\Pi = \Pi^{\mathrm{M}} + \Pi^{\mathrm{I}} \tag{13}$$

$$= \sum_{j=1}^{N}\alpha + \sum_{i=1}^{N}\sum_{j\neq i}\boldsymbol{\alpha}_i \cdot \mathbf{T}(r_{ij}) \cdot \boldsymbol{\alpha}_j \tag{14}$$

in which $\mathbf{T}(\mathbf{r})$ is the dipole tensor. The connection of the macroscopic measurement (11) to the molecular information is made through equations (13) and (14), although for highly polarizable molecules higher-order terms should be included in equation (14). Inclusion of the intermolecular component of Π yields three contributions to the measured Ψ_{xz}, arising from (a) molecular reorientation, (b) the intermolecular (or interaction-induced) component and (c) a cross-term between these two [61, 62]. In general these three components all contribute to the OHD-OKE signal, although the number of components may be reduced by symmetry. For example, for atoms and spherically symmetric molecules, such as CCl_4, orientational motion will not contribute to the signal. An important objective of the analysis of the OHD-OKE data is to characterize these contributions separately. It has been pointed out by

Ladanyi and Liang that the interaction-induced component relaxes by both orientational and translational motion [62]. The former will relax with the same dynamics as (a), rendering the separation desired difficult to achieve. They showed that by using a method of projected variables a more meaningful separation into orientational and translational dynamics can be achieved [61, 62].

OHD-OKE data have now been recorded for a large number of pure liquids, revealing many common features. At time zero there is a symmetric instantaneous response which reflects the laser autocorrelation. This arises from the electronic hyperpolarizability $\sigma(t)$. Beyond that an ultrafast (subpicosecond) approximately exponential relaxation and a strongly damped oscillatory feature contribute to the fastest nuclear dynamics. On the longer (greater than 1 ps) timescale the relaxation is well described by a sum of two exponentials, one in the range 0.5–5 ps and one in the range 5–100 ps. These features are all apparent in figure 3. In addition a rapid, underdamped, oscillatory component is often observed.

It is common practice, somewhat justified by the results of molecular dynamics (MD) simulation [65], to treat separately the longest exponential relaxation time. This component is assigned to diffusive molecular reorientation. Some quite detailed attempts have been made to analyse the relaxation times in terms of the Debye model of orientational relaxation [42, 47, 49], which predicts, for a molecule represented by an ellipsoidal shape with two equal axes [57–59],

$$\tau_r = \frac{V_{eff}\eta}{kT} + \tau_r^0 \tag{15}$$

in which η is the viscosity and τ_r^0 the reorientation time at zero viscosity. The effective volume is given by $V_{eff} = VfC$ where V is the molecular volume, f a shape factor and C a shape-dependent factor which depends on whether a slip or stick boundary condition is assumed. Both depend on the axial ratio of the ellipsoid and may be calculated or are tabulated [66–69]. For an ellipsoid with three unequal axes the orientational dynamics is more complex, yielding multiexponential relaxation [57–59]. The orientational relaxation time measured in the OHD-OKE experiment is a collective time, τ_c, whereas the Debye relaxation time refers to a single molecule. The two are connected by [59]

$$\tau_c = \frac{g_2}{j_2}\tau_r \tag{16}$$

in which g_2 is a measure of static orientational correlations between pairs of molecules and j_2 accounts for dynamic angular momentum correlations. The latter is believed to take a value close to unity in most circumstances [59]. The former will tend to unity with increasing dilution in non-interacting solvents.

In figure 6 we plot the τ_c data for nitrobenzene measured as a function of (a) temperature in the neat liquid, (b) temperature in a 10% solution in heptane and (c) dilution in heptane, against η/T (equation (15)). The linear concentration-independent relationship found in all cases is strong evidence for a diffusive reorientation and suggests that g_2 is close to 1 in this molecule. Similar results were obtained for benzonitrile [47]. A value of g_2 close to 1 for these polar molecules suggests that orientational correlation is less influenced by dipole moment than other factors (for example molecular shape). The measured value of V_{eff} is not in exact agreement with calculations, but this may reflect a number of approximations that have to be made in the analysis (ellipsoidal shape, slip boundary condition, negligible

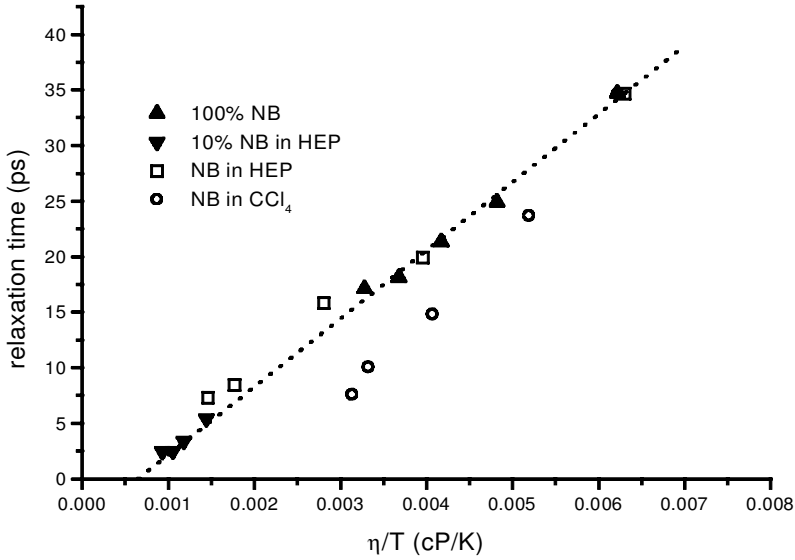

Figure 6. Plot of the slowest relaxation time for nitrobenzene, τ_c, as a function of temperature and dilution [47]. That the points lie on a single line strongly suggests that $g_2 = 1$. The data for CCl_4 are somewhat anomalous, in that they lie below the other data and have a large negative τ^0. This may arise from solvent–solute complex formation [11].

contribution to τ_c of dielectric friction, ...). Interestingly the assumptions which yield the best agreement between calculated and measured V_{eff} also predict that the orientational relaxation time should be near to monoexponential. As noted above, this is not observed to be the case; an additional relaxation time of a few picoseconds is also invariably recovered. Under other assumptions about molecular shape the modified Debye model indeed predicts a multiexponential relaxation [57]. However, there are no reasonable models of molecular shape which yield a relaxation time which is a factor of 10 shorter than the long relaxation time, as observed experimentally [47]. It has therefore to be concluded that the shorter of the two exponential relaxation times observed cannot be assigned to diffusive reorientation. We shall return to the discussion of this second exponential component below.

The assignment of the ultrafast features is often more transparent in the frequency domain. An example of the ultrafast spectral density, $\mathrm{Im}[D'(\omega)]$, was shown in figure 5. The ultrafast spectral density is constructed by subtracting from the time domain data the function

$$r_1(t) = \left[\sum_i a_i \exp(-t/\tau_i)\right][1 - \exp(-2\omega_0 t)], \tag{17}$$

where the second term represents an inertial rise time, with ω_0 being taken from the mean frequency of the ultrafast spectral density [27]. The same subtraction can be accomplished in the frequency domain [33]. This removes the long-time (or low-frequency) response which characterizes the diffusive dynamics (compare figures 4 and 5).

The ultrafast spectral density so recovered typically reveals a multicomponent lineshape. Narrow bands at higher energy (greater than 200 cm^{-1} in figures 4 and 5) can often be assigned, on the basis of gas-phase vibrational spectra, to intramolecular modes. The broad low-frequency band seen in figure 5 is of most interest in liquid dynamics studies, because it reflects the intermolecular interactions. Clearly this low-frequency lineshape is complex and cannot be represented by a single Gaussian or Lorentzian function. This is as expected from the preceding discussion, in which distinct single-molecule and interaction-induced contributions to $r(t)$ were identified. Clearly some means of deconvoluting these contributions is desirable, and this inevitably involves a degree of curve fitting. Chang and Castner [38], in a procedure subsequently adopted by a number of groups [33, 41, 44, 45, 47, 55], showed that $\mathrm{Im}[D'(\omega)]$ can often be well represented by the sum of an antisymmetrized Gaussian

$$I_{\mathrm{G}}(\omega) = g_1\left(\exp\left\{\frac{-2(\omega-\omega_1)^2}{\Delta\omega^2[2\ln(2)]^{-1}}\right\} - \exp\left\{\frac{-2(\omega+\omega_1)^2}{\Delta\omega^2[2\ln(2)]^{-1}}\right\}\right) \tag{18}$$

and the generalized Ohmic lineshape [70], related to the Bucaro–Litovitz (BL) function [71]

$$I_{\mathrm{BL}}(\omega) = b\omega^{\alpha}\exp\left(-\frac{\omega}{\omega_{\mathrm{BL}}}\right). \tag{19}$$

In these the fitting parameters are the Gaussian halfwidth $\Delta\omega$, the Gaussian frequency ω_1, the BL frequency ω_{BL}, the exponent α and the relative amplitude g_1/b. Although this fitting procedure is partly empirical (see below), this pair of functions has been remarkably successful at describing the ultrafast spectral densities of a large number of liquids [33, 38, 39, 41, 44, 45, 47, 55].

Other descriptions of $\mathrm{Im}[D'(\omega)]$ have been used. An analysis in terms of a hierarchy of underdamped, critically damped and overdamped oscillators was proposed by McMorrow and coworkers [72] and applied to liquid CS_2 [35]. A closely related approach was described by Mukamel and coworkers, who suggested that $\mathrm{Im}[D(\omega)]$ could be described by a series of Brownian oscillators (BOs) [63, 73]:

$$\mathrm{Im}[D(\omega)] = \sum_i \frac{\omega\eta_i\kappa_i}{2\pi[(\omega_i^2-\omega^2)^2+\omega^2\gamma_i^2]}. \tag{20}$$

In equation (20) ω_i is the frequency of the ith mode, κ_i is the coupling strength and γ_i is the damping (the friction induced by the heat bath on the ith oscillator). The attractive feature of this approach is that a single function scales between a Lorentzian lineshape (strongly damped, $\gamma_i \gg \omega_i$) characteristic of diffusive reorientation and a Gaussian, for an undamped ($\gamma_i = 0$) mode, under the assumption of a Gaussian distribution of coupling strengths. The BO analysis has been successfully applied to $\mathrm{Im}[D'(\omega)]$ for acetonitrile [74], H_2O [36], and iodobenzene [49].

We have compared the fit of equation (20) ($i = 2$) with that for equations (18) + (19) to $\mathrm{Im}[D'(\omega)]$ for aniline, nitrobenzene and benzonitrile. Invariably equations (18) + (19) gave a better fit [47]. In general equation (20) fails on the high-frequency side of the spectral density, because it does not return to the baseline. We have also compared equations (18) + (19) with multiple Gaussian functions, as may be appropriate for multiple underdamped modes. Again, for the aromatic liquids we have studied, the fit of equations (18) + (19) is invariably superior.

The justification for the assumption of a Gaussian component (18) in $\mathrm{Im}[D'(\omega)]$ is quite sound. On an ultrafast timescale the single-molecule contribution mentioned above will take the form of a hindered molecular reorientation, or librational, motion. Lynden-Bell and Steele [75] proposed a Gaussian cage model to describe librational motion in liquids. In that model a molecule is taken to be located in a cage formed by its neighbours. The molecule undergoes orientational motion, until reaching the edge of the cage, where the torque acting upon it tends to reverse its angular momentum. This reversal can lead to oscillatory behaviour, as often observed in $r(t)$. In the Lynden-Bell–Steele model the molecular motion is assumed to be harmonic and the distribution of cage structures is assumed to yield a Gaussian distribution of harmonic frequencies. This is the purely inhomogeneously broadened limit of the lineshape. More realistically, fluctuations in the frequency due to fluctuations in cage structure are expected, and this introduces a homogeneously broadened component [75].

It would clearly be of great interest to separate the inhomogeneous, structural, and homogeneous, dynamic, contributions to the liquid lineshape. Unfortunately this turns out not to be possible in OHD-OKE measurements, which have only a single time dimension (the pump–probe delay) [73, 74], although some progress can be made by studying the temperature dependence [36]. It has been shown that such a separation is, in principle, possible in temporally two-dimensional experiments [74]. The best known of these is the three-pulse photon echo [76], but the difficulties of performing this experiment at the far-IR frequencies required are considerable. Alternative six-wave mixing experiments have been proposed [73, 77–80]. Resonant six-wave mixing experiments have been demonstrated for studies of solute dynamics [81, 82], but the non-resonant multidimensional experiments required to unravel the ground-state dynamics of liquids have proved challenging, in particular because the six-wave signal is polluted by contributions from cascaded lower-order signals [83, 84]. However, progress in overcoming this problem has recently been reported, and it seems likely that these challenging measurements will provide important new information in the near future [85]. Further discussion of the subject is, however, both temporally and thematically beyond the scope of the current review.

The assignment of the Gaussian component of $\mathrm{Im}[D'(\omega)]$ to a librational mode of the liquid has been investigated in a quantitative fashion [47]. In the harmonic model the potential as a function of the angle of reorientation θ will be

$$V(\theta) = \tfrac{1}{2}k\theta^2 \tag{21}$$

where k is the force constant,

$$k = \omega_1^2 I, \tag{22}$$

in which ω_1 is the librational frequency and I is the moment of inertia. Thus the observed frequency of librational motion should scale as $(k/I)^{1/2}$. In general k is not known. Smith and Meech [47] measured ω_1 for benzonitrile and two of its *para*-substituted derivatives and assumed that the similar shapes and intermolecular interactions in the series would yield a constant value of k. It was found that the shift of ω_1 was in the direction predicted, and the magnitude of the shift scaled with $I^{-1/2}$. However, the shift observed was somewhat larger than predicted on the basis of equation (22). Neelakandan *et al.* showed that the observed librational frequencies of benzene and hexafluorobenzene could be well understood on the basis of the harmonic model [44]. In addition they showed that the librational frequency of 1,3,5-

trifluorobenzene could also be understood on the basis of the model, if predicted changes in the liquid structure of the tri-substituted derivative were taken into account. Kamada *et al.* measured the librational frequencies for the series furan, thiophene and selenophene [55]. They calculated a value for k based on the free volume of the liquids. The agreement between the predictions of the harmonic model and observations were good for furan and thiophene. This accumulation of data is probably sufficient to conclude that the Gaussian component can in many cases be assigned to a librational mode of the liquid. However, it should be noted that there are data which do not fit this simple picture. The selenophene data in the study of Kamada *et al.* reverse the trend predicted by the harmonic model [55]. The series of three halobenzenes studied by Friedman and She also reveal a trend which is the opposite to that expected (if it is assumed that k is similar in the three liquids) [30]. Finally, H-bonded aromatic liquids (including benzoyl alcohol [41], pyrrole [52] and aniline [33, 45]) yield particularly high values of ω_1. Whether such departures from the model indicate serious shortcomings, or simply the need for a better estimate of k, is not clear at present.

In addition to the Gaussian component it is often observed that the ultrafast spectral density has an initial rapid rise in intensity, which drops off at higher frequency. In many cases this is manifested as a low-frequency shoulder in $\mathrm{Im}[D'(\omega)]$ (figure 5). This component is well represented by the function I_{BL} (equation (19)), so called because a form of it, with specific values of α, was derived by Bucaro and Litovitz to described the low-frequency, collision-induced, DLS spectra of non-polar spherically symmetric atomic and molecular liquids [71]. The function is also called the generalized Ohmic lineshape (from the Ohmic lineshape, for which $\alpha = 1$) [70].

In this sense the I_{BL} lineshape could be thought to account for some of the non-single-molecule contributions to $\mathrm{Im}[D'(\omega)]$. However, I_{BL} was originally derived on the basis of the short-range isolated binary collision model for intermolecular interactions. The interaction-induced components of $\mathrm{Im}[D'(\omega)]$, described by equation (14), are of a more general and long-range type. Unfortunately, because of the strong dependence of equation (14) on intermolecular distance and orientation it is very difficult to propose a closed form for the interaction-induced lineshape in molecular liquids. However, the lineshape can be calculated from the results of molecular dynamics simulations. The simulations of Ladanyi and coworkers [62, 86] for acetonitrile showed that the interaction-induced terms contribute at all times (frequencies), not just at low frequency, as might be concluded from the typical behaviour of I_{BL}.

It has been suggested that the component represented by I_{BL} may arise from low-frequency modes of specific (albeit transient) structures in the liquid. For example McMorrow and coworkers assigned the low-frequency shoulder observed in the spectral density of liquid benzene (which is well fitted by equation (19) [44]) to a dimer structure [27]. They reported that the shoulder disappeared on dilution of benzene in $CHCl_3$, consistent with a shift in a monomer–dimer equilibrium. A similar change in $\mathrm{Im}[D'(\omega)]$ was observed for the dilution of benzonitrile in isopentane [47], but the apparent disappearance of the shoulder may simply be a result of its merging with the Gaussian band, which shifts down in frequency (see below). The assignment of the low-frequency part of $\mathrm{Im}[D'(\omega)]$ of benzene to a dimer is supported by the observation of bands at the relevant frequencies in gas-phase spectroscopy of jet-cooled benzene dimers [87]. It is also noteworthy that there is a wide variation in the relative contributions of equations (18) and (19) to $\mathrm{Im}[D'(\omega)]$,

both for different liquids and even within a series of similar liquids [54]. This might also indicate that vibrational or librational modes of short-lived intermolecular complexes contribute to this part of $\mathrm{Im}[D'(\omega)]$. Thus, the intermediate-frequency component of $\mathrm{Im}[D'(\omega)]$, which is very well fitted by equation (19), is not completely understood. There may be contributions from collision- and interaction-induced intermolecular interactions, as well as from modes associated with local transient liquid structures.

The remaining part of the spectral density to be discussed is the shorter of the two exponential relaxation times, which has often been included in the diffusive response, and is therefore subtracted from the ultrafast spectral density. One thing that can be asserted with confidence is that this component does not arise from diffusive reorientation. First, the fast component is observed in liquids comprising molecules which are predicted to exhibit a rigorously monoexponential diffusive relaxation [54]. Second, for less symmetric molecules, where multicomponent orientational relaxation is expected [57], the relaxation time observed is much smaller than predicted by the modified Stokes–Einstein–Debye equation [47].

A number of groups have assigned the fast exponential component to the relaxation of short-lived structures in the liquid, that is a relaxation intermediate between librational dephasing and collective reorientational motion [47, 49]. However, few details were given on the nature of this short-lived structure, and it is surprising that this structural feature should be seen in such a very wide variety of liquids, and with a rather similar relaxation time. Recently a very detailed investigation of the fast exponential relaxation time was made as a function of temperature for six symmetric top liquids [54]. A strong correlation between the fast relaxation time and the slower, truly diffusive, relaxation was observed. This result suggests that the fast relaxation time is proportional to the rate of orientational diffusion (for liquids in which $g_2 = 1$) [54]. It was proposed that the fast relaxation time arises from spectral diffusion, arising from structural fluctuations, reflected by τ_c. The quality and quantity of data in support of this mechanism are already impressive [54]. Some additional data are collected in figure 7 which shows a scatter plot of the fast and slow (τ_c) exponential relaxation times for a series of aromatic liquids, measured in three different laboratories. Although the correlation of fast and slow relaxation times is not as strong as that reported by Loughnane *et al.*, it is still good. This represents further support for the motional narrowing model [54].

To summarize this section, the spectral densities of a number of pure liquids have been determined with high accuracy using the OHD-OKE method. The spectral densities reveal complex lineshapes. One simple approach to the analysis is to break these down into a sum of simpler lineshapes. This procedure allows a good fraction of the spectral density to be assigned. There is quite persuasive evidence that the high-frequency, Gaussian, component can be assigned to librational motion. Similarly the lowest-frequency data are readily assigned to diffusive orientational motion. The difficulty lies in the intermediate-frequency region. The recent assignment of the fast exponential relaxation to motional narrowing [54] is well supported by a range of data. The assignment of the component fit by I_{BL} remains unclear. Certainly the amplitude of this component changes greatly from liquid to liquid, in a way which is difficult to predict. It may be that I_{BL} serves as a fitting function to represent 'the rest': collision induced, interaction induced, modes due to local liquid structure, etc. Further work is required to resolve the unsatisfactory state with regard to the intermediate-frequency region of $\mathrm{Im}[D(\omega)]$ in pure liquids.

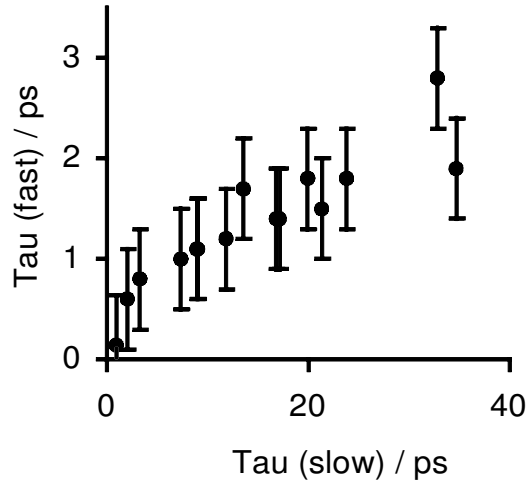

Figure 7. Scatter plot of fast and slow exponential relaxation times for aromatic liquids (following [54]). Data taken from Smith *et al.* [45, 47], Kamada *et al.* [55] and Neelakandan *et al.* [43, 44]. Error bars are an estimated ±0.5 ps for the fast component. No error bars are included for the long relaxation time, although it should be noted that its accurate determination requires measurements over several lifetimes.

3.2. *Mixed liquids*

There are at least two motives for studying liquid mixtures. The first is to characterize better the dynamics of the pure liquid, by, for example, using dilution to minimize interaction-induced contributions to the lineshape. In this case a 'non-interacting' solvent is often chosen as the second component, ideally one which hardly contributes to the OHD-OKE signal. The second motive is to understand better the dynamics of liquid mixtures themselves, in which case the most interest is in components which interact strongly.

Dilution is an established means of investigating the contribution of orientational pair correlation, g_2, to the collective orientational relaxation time, τ_c [59]. The expectation is that as the concentration of the solute tends to zero then g_2 approaches 1 and $\tau_c = \tau_r$. Smith and Meech recorded τ_c for two aromatic liquids on dilution in isopentane, and found that $\tau_c \propto \eta$, consistent with $g_2 = 1$ [47]. On the other hand Idrissi *et al.* studied CS_2 in CCl_4 and observed that τ_c was a function of composition even at constant η [50]. This result suggests a finite and composition dependent g_2 in this mixture. Kamada *et al.* investigated the orientational relaxation time of thiophene in CCl_4 [11]. An unexpected maximum in τ_c was observed, which was interpreted as arising from the formation of a solvent–solute complex. This was supported by the observation of changes in the electronic absorption spectrum of the solute on dilution.

The effect of dilution in non-interacting solvents on the ultrafast spectral density has also been investigated. For CS_2, nitrobenzene and benzonitrile the effect of dilution is broadly the same, a shift of $\mathrm{Im}[D'(\omega)]$ to lower frequency, accompanied by spectral narrowing. An example is shown in figure 8. The difficulties encountered in separating homogeneous/inhomogeneous and librational/interaction-induced contributions to the lineshape make the interpretation of this result problematic. McMorrow *et al.* [35] and later Smith and Meech [47] noted that surrounding a polar

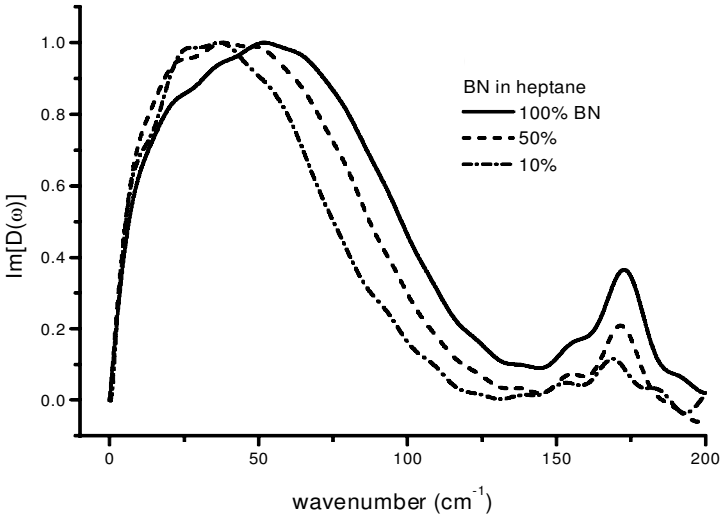

Figure 8. Plots of $\mathrm{Im}[D'(\omega)]$ for benzonitrile on dilution in heptane. Note the shift to lower wavenumber and narrowing of the spectral density.

or polarizable solute with a non-polar solvent will lead to a change in the force constant for the librational motion. This is consistent with the observed shifts to lower frequency. The narrowing of the spectral density could be thought to imply reduced inhomogeneous broadening in the solution, arising from a narrower site distribution. However, McMorrow *et al.* found that a similar narrowing could arise from an increase in the rate of damping of the oscillator [35]. Conversely Steffen *et al.*, who also studied CS_2 diluted in non-polar solvent, suggested that the concentration dependence of $\mathrm{Im}[D'(\omega)]$ was more consistent with the elimination of interaction-induced components on dilution [53]. There appears to be insufficient information in the data to separate these explanations. This is one area in which the two-dimensional experiments alluded to above are likely to be of great value.

Liquids comprising two strongly interacting molecules have been studied in a few cases. The signature of a significant effect of intermolecular interaction on the liquid-state dynamics is the observation of non-additivity in the ultrafast data, i.e. the solution spectral density cannot be fit by the weighted sum of its components. This method was originally applied by Chang and Castner in their study of formamide–water and formamide–acetonitrile solutions, in which dilution was found to have a significant effect on intermolecular structure [37]. Neelakandan *et al.* observed non-additivity in mixtures of benzene and hexafluorobenzene, possibly indicative of the formation of complexes [43].

3.3. *Liquid-state dynamics and reactions in solution*

Liquid-state dynamics are believed to have a pronounced effect on the rates of chemical reactions in solution and are one of the origins of the profound differences between liquid-phase and gas-phase reactivity. Much experimental and theoretical work has focused on electron transfer reactions, where it has been suggested that the liquid dynamics exercise a rate-controlling effect [88–90]. However, it is difficult to make a simple connection between electron transfer rate and liquid dynamics, because the former often involves the rate of diffusion and mutual orientation of

electron donor and acceptor (although the effect of diffusion can sometimes be removed by choosing a solvent which acts also as the electron donor [91, 92]). A more convenient comparison can be made between liquid-state dynamics and the dynamics of solvation. Dipole solvation is readily observed through the time evolution of the fluorescence spectrum of a solute which exhibits a change in dipole moment on electronic excitation [93]. A simple continuum picture of the solvent predicts that solvation should occur in the timescale τ_L of the longitudinal dielectric relaxation time of the pure liquid [93]. Early picosecond time-resolved measurements found that solvation did occur on the timescale of τ_L, but with significant deviations, which already suggested the need for more realistic models [94, 95]. Subsequent ultrafast measurements and MD simulations showed that a substantial fraction of the solvation dynamics occurred much faster than τ_L [96–98]. The MD data were particularly important, as they suggested that the dominant microscopic mechanism of dipole solvation was solvent reorientation about the changed dipole moment of the solute [96].

Cho *et al* [99] were the first to suggest that OHD-OKE data could be used to model the ultrafast solvation times, and their approach was successful in reproducing the ultrafast (faster than τ_L) dynamics of solvation reported by Rosenthal *et al.* [98]. At the same time Maroncelli and coworkers proposed, on the basis of MD simulations, that the solvation time correlation function $C_V(t)$ was directly related to the dipole correlation function $C_1(t)$, measured in dielectric relaxation experiments,

$$C_V(t) = [C_1(t)]^{\alpha_S} \tag{23}$$

where α_S is a solvent-dependent constant [100]. Thus, were $C_1(t)$ readily available from dielectric relaxation data there would be no obvious role for the OHD-OKE measurement in simulating solvation dynamics. Unfortunately there are severe experimental difficulties involved in making dielectric relaxation (or far-IR) measurements at the frequencies required to model solvation dynamics. Thus it is desirable to have a means of connecting the $C_1(t)$ required for solvation dynamics to the $C_2(t)$ measured, with high resolution, in OHD-OKE. The method, first outlined by Chang and Castner [38], is to construct $C_2(t)$ by numerical integration of $r(t)$ (equation (11))

$$C_2(t) = 1 - \int_0^t r(t)\,\mathrm{d}t \Big/ \int_0^\infty r(t)\,\mathrm{d}t \tag{24}$$

where $r(t)$ is obtained deconvoluted and with high signal to noise by the inverse Fourier transform of $\mathrm{Im}[D(\omega)]$ (equation (10)). In the limit that $r(t)$ is dominated by orientational dynamics (i.e. the interaction-induced contribution is negligible) then $C_1(t)$ is recovered from [38]

$$C_1(t) = [C_2(t)]^{1/3}. \tag{25}$$

Thus, using equations (23)–(25) it is possible to simulate the solvation dynamics of essentially any liquid for which OHD-OKE data have been obtained. The results for several liquids were discussed by Chang and Castner [38, 41]. Smith *et al.* made a direct comparison between the predictions of equations (23)–(25) and the experimentally determined $C_V(t)$ for liquid aniline, a solvent of importance in the study of ultrafast electron transfer reactions [45, 101]. The results are shown in figure 9. The broad features of the solvation dynamics data are well reproduced by the simulation, with fast and slow components being found in both cases, of approximately the

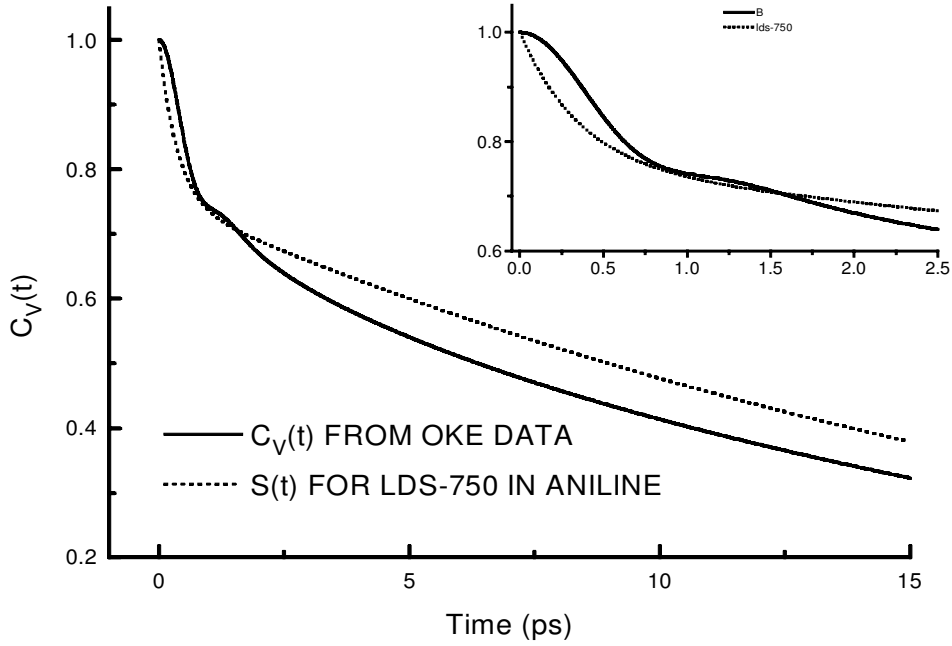

Figure 9. A comparison of the calculated $C_V(t)$ for liquid aniline. The calculated curve was recovered from the data in figures 3 and 4. The measured data were taken from ultrafast fluorescence up-conversion measurements of the dynamic Stokes shift of the dye LDS-750 in aniline [102].

correct magnitude and weight. This leads to the conclusion that ultrafast solvation dynamics arise from solute librational motion, as this is the dominant component of $\mathrm{Im}[D'(\omega)]$ (figure 5). However, there are differences in detail between the solvation measurement and the predictions from the OHD-OKE data. In particular the Gaussian shape of the calculated response at early times is not observed. This may reflect difficulties in the time resolution and signal to noise of solvation dynamics measurements, or it could arise from a broader distribution of librational frequencies in the solution, compared with the pure liquid, especially when it is realized that dynamics in the first and second solvation shells have a dominant effect on solvation [96, 97]. Maroncelli and Castner reported a comprehensive survey of solvation dynamics, dielectric relaxation and OHD-OKE dynamics, and the connections between them, using data for more than twenty solvents [103]. They found that in general the simulation of solvation dynamics from dielectric relaxation data was more successful than that from OHD-OKE, although some assumptions about the form of the dielectric relaxation data on the 0–1 ps timescale were required. The relative failure of the OHD-OKE data to reproduce $C_V(t)$ can be attributed to the contribution of interaction-induced components in OHD-OKE data, which are of less significance in solvation dynamics, where orientational motion appears to make the dominant contribution. The Maroncelli and Castner article [103] also contains a useful discussion of the power law relations exemplified by equations (23) and (25), developed by Raineri and Friedman [104]. Such relations are a powerful means of relating the dynamics observed in one experiment to those found in another.

OHD-OKE data have been used to simulate the results of other ultrafast experiments. For example Vöhringer *et al.* used $\mathrm{Im}[D(\omega)]$ as input to simulate two-pulse photon echo measurements of optical dephasing in solution [105]. The approach was contrasted with that of fitting the echo data to a sum of overdamped Brownian oscillators. Both approaches were successful in describing the data, but the use of an experimentally determined parameter, $\mathrm{Im}[D(\omega)]$, allowed an assessment of the solvent–solute interaction mechanism. Vöhringer *et al.* observed that the solvent–solute coupling, derived from the fit to the echo data, scaled with solvent polarizability, as did the solute electronic absorption frequency. Thus this is a case where the most significant intermolecular interactions involve molecular polarizability, rather than polarity. In such cases the OHD-OKE data are likely to be particularly well suited to analysing solution phase dynamics.

3.4. *Dynamics in heterogeneous and ordered systems*

It has been seen that the OHD-OKE experiment is already a mature one with regard to studies of the homogeneous liquid phase. More recently the experiment has been applied to heterogeneous systems, most notably the dynamics of liquids in porous glasses and the dynamics of liquid crystals.

An extensive investigation of the dynamics of liquids in sol–gel glasses of varying but known pore size has been presented by Fourkas and coworkers [17, 106–108]. For the non-wetting liquid CS_2 the orientational relaxation time was found to be non-exponential, with one component reflecting a bulk-like phase, and one which was more than an order of magnitude slower. The slower relaxation time was dependent on the size of the pores [107]. Detailed analysis showed that the retarded relaxation time arose from a surface layer less than one molecule thick, and the retardation was accounted for by geometrical confinement. Interestingly $\mathrm{Im}[D'(\omega)]$ was unaltered by confinement.

A slightly different picture was found in a study of confined liquid acetonitrile, which does wet the surface [108]. Again a surface layer was found to have a strongly retarded orientational relaxation time. However, replacement of the surface H-bond population by methylation showed that H-bond donation from the surface was the primary mechanism restricting orientational motion at the interface. In addition an intermediate relaxation time was detected, which was analysed in terms of fast exchange between the surface-restricted and bulk-like populations.

Several groups have investigated the orientational dynamics of liquid crystals. In all cases an extremely broad distribution of relaxation times was reported. For example Stankus *et al.*, using a transient grating OKE method, found relaxation times in the liquid crystal MBBA ranging from picoseconds to tens of nanoseconds [109]. For the longer relaxation times the temperature dependence was interpreted in terms of Landau–de Gennes theory. Intermediate and fast relaxation times were discussed in terms of the relaxation times of local structures in the liquid crystal, which was in the isotropic phase. Similar results were found for pentylcyanobiphenyl liquid crystal [110]. This type of measurement was extended to the cyanocyclohexyl liquid crystal ZLI-1167 by Torre and coworkers [111]. In addition to these measurements of the isotropic phase LeCalvez *et al.* reported an OKE study of cyanobiphenyl in the smectic A phase. The dynamics reflect librational and diffusive reorientation and reveal the existence of strong intermolecular interactions [112].

The above measurements suggest that the extremely high time resolution and signal-to-noise ratio available from the ultrafast OHD-OKE experiment could find

application in recording the fastest dynamics in media which are considerably more complex than the homogeneous liquids usually studied. Other examples include the study of monomer–polymer dynamics by Shirota and Castner [113] and measurements on colloidal suspensions [114]. The only limiting factor in the choice of system to be studied is the requirement for a sample of high optical quality.

4. Summary

In summary, the OHD-OKE provides a relatively straightforward route to the measurement of the ultrafast dynamics of a variety of transparent media. The principles and practice of the OHD-OKE measurement have been described. With the aid of the recent generation of stable ultrafast lasers, careful control of polarization and samples of good optical quality the experiment provides transient data with extremely good signal-to-noise ratios. The Fourier transform analysis methods, also described, are now well established and provide the Raman spectral density in the frequency domain $\mathrm{Im}[D(\omega)]$ or the nuclear dynamics in the time domain $r(t)$, undistorted by the finite pulsewidth of the laser. These traces are well suited to subsequent analysis.

The Raman spectral density has been measured for a large number of liquids. For many a number of characteristic features are found. An approximately Lorentzian component at zero frequency is well described by hydrodynamic models of diffusive orientational relaxation. A component at higher frequency of Gaussian shape can be assigned to librational motion. At still higher frequencies intramolecular Raman-active modes are observed, but these are seldom of principal interest. The origin of the intensity in the spectral density at frequencies intermediate between the diffusive Lorentzian and Gaussain librational component is less transparent. It seems highly likely that a second, broader, Lorentzian component can be assigned to spectral diffusion arising from structural fluctuations in the liquid, particularly orientational motion. However, for many polarizable molecules one expects a contribution to the spectral density from interaction-induced effects. These may indeed contribute at the intermediate frequency but are expected to be significant over a broad frequency range. Finally, specific intermolecular structures in the liquid may have intermolecular modes at these frequencies. Despite these uncertainties, substantial fractions of the Raman spectral densities of many molecular liquids can be assigned.

The high-resolution picture of liquid dynamics available from OHD-OKE experiments has led to their being used as input to simulations of other ultrafast optical measurements. In some cases it has proved possible to simulate measurements of solvation dynamics, but in general a direct measurement of the liquid's dipole correlation function $C_1(t)$ is preferable. This is because the polarizability relaxation measurement, which the OHD-OKE yields, contains a contribution from interaction-induced effects which are not significant in solvation, where dipole reorientation dominates. OHD-OKE data have, however, proved useful in simulating optical lineshapes derived from photon echo experiments.

Recently a number of groups have sought to exploit the capabilities of the OHD-OKE method to extract information on the dynamics of complex heterogeneous media. New data have been recorded for liquids confined in porous glasses and for liquid crystals. There seems no reason why the method should not be extended to solutions of polymers or dendrimers and to colloidal media. The principal experimental limitation is the need for high-quality optical samples.

There are limitations on the data that can be extracted from measurements with a single time delay (or dimension), such as the OHD-OKE. In particular it is impossible to separate homogeneous and inhomogeneous contributions to the spectral density. Such a separation is in principle possible with two-dimensional multipulse experiments. The price, at least with currently available technology, is an increase in experimental complexity. However, in recent years there has been rapid progress in multidimensional spectroscopy, and it seems certain that it will shortly be possible to provide further details on liquid dynamics using these methods. That may, however, turn out to be a relatively minor application of these powerful new methods, which seem capable of yielding data on the structural dynamics of even moderately complex molecules. These will no doubt become the topics of future reviews.

Acknowledgment

We are grateful to the Engineering and Physical Sciences Research Council for financial support and the award of a studentship to N.A.S.

References

[1] Kerr, J., 1875, *Phil. Mag.*, **50**, 337.
[2] Buckingham, A. D., 1956, *Proc. Phys. Soc.*, **B69**, 910.
[3] Mayer G., and Gires, F., 1964, *C. R. Acad. Sci. (Paris)*, **258**, 2039.
[4] Maker, P. D., and Terhune, R. W., 1964, *Phys. Rev. Lett.*, **12**, 507.
[5] Jenkins, F. A., and White, H. E., 1981, *The Fundamentals of Optics* (Singapore: McGraw-Hill).
[6] Kirkwood, J. C., Ulness, D. J., and Albrecht, A. C., 2000, *J. phys. Chem.* A, **104**, 4167.
[7] Levenson, M. D., and Kano, S. S., 1988, *Introduction to Nonlinear Laser Spectroscopy* (New York: Academic Press).
[8] Tang, C. L., 1997, *J. nonlinear Optics Phys. and Mater.*, **6**, 535.
[9] Riedle, E., Beutter, M., Lochbrunner, S., Piel, J., Schenkl, S., Spörlein, S., and Zinth, W., 2000, *Appl. Phys.* B, **71**, 457.
[10] Kafka, J. D., and Baer, T., 1987, *Optics Lett.*, **12**, 401.
[11] Kamada, K., Ueda, M., Sakaguchi, T., Ohta, K., and Fukumi, T., 1996, *Chem. Phys. Lett.*, **249**, 329.
[12] Fleming, G. R., 1986, *Chemical Applications of Ultrafast Spectroscopy* (Oxford: Oxford University Press).
[13] Palese, S., Schilling, L., Miller, R. J. D., Staver, P. R., and Lotshaw, W. T., 1994, *J. phys. Chem.*, **98**, 6308.
[14] Sala, K., and Richardson, M. C., 1975, *Phys. Rev.* A, **12**, 1036.
[15] Cho, M., Du, M., Scherer, N. F., Fleming, G. R., and Mukamel, S., 1993, *J. chem. Phys.*, **99**, 2410.
[16] Kinoshita, S., Kai, Y., Ariyoshi, T., and Shimada, Y., 1996, *Int. J. mod. Phys.* B, **10**, 1229.
[17] Farrer, R. A., Loughnane, B. J., and Fourkas, J. T., 1997, *J. phys. Chem.* A, **101**, 4005.
[18] Lotshaw, W. T., McMorrow, D., Thantu, N., Melinger, J. S., and Kitchenham, R., 1995, *J. Raman. Spectrosc.*, **26**, 571.
[19] Alavi, D. S., Hartman, R. S., and Waldeck, D. H., 1990, *J. chem. Phys.*, **92**, 4055.
[20] Cross, A. J., Waldeck, D. H., and Fleming, G. R., 1983, *J. chem. Phys.*, **78**, 6455.
[21] McMorrow, D., Lotshaw, W. T., and Kenney-Wallace, G. A., 1988, *IEEE J. quantum Electron.*, **24**, 443.
[22] Lotshaw, W. T., McMorrow, D., and Kenney-Wallace, G. A., 1988, *Proc. SPIE* **981**, 20.

[23] McMorrow, D., and Lotshaw, W., 1990, *Chem. Phys. Lett.*, **174**, 85.
[24] McMorrow, D., and Lotshaw, W., 1991, *Chem. Phys. Lett.*, **178**, 69.
[25] McMorrow, D., and Lotshaw, W., 1991, *J. phys. Chem.*, **95**, 10395.
[26] Back, R., Kenney-Wallace, G. A., Lotshaw, W. T., and McMorrow, D., 1992, *Chem. Phys. Lett.*, **191**, 423.
[27] McMorrow, D., and Lotshaw, W., 1993, *Chem. Phys. Lett.*, **201**, 369.
[28] Kinoshita, S., Kai, Y., Yamaguchi, M., and Yagi, T., 1995, *Phys. Rev. Lett.*, **75**, 148.
[29] Cong, P., Simon, J. D., and She, C. Y., 1996, *J. chem. Phys.*, **104**, 962.
[30] Friedman, J. S., and She, C. Y., 1993, *J. chem. Phys.*, **99**, 4960.
[31] Nielsen, O. F., 1994, *Annu. Rep. Proc. Chem.*, C **91**, 3.
[32] Kamada, K., Ueda, M., Sakaguchi, T., Ohta, K., and Fukumi, T., 1996, *Chem. Phys. Lett.*, **263**, 215.
[33] Smith, N. A., Lin, S., Meech, S. R., Shirota, H., and Yoshihara, K., 1997, *J. phys. Chem.* A, **101**, 9578.
[34] Greene, B. I., Fleury, P. A., Carter, H. L., Jr., and Farrow, R. C., 1984, *Phys. Rev.* A, **29**, 271.
[35] McMorrow, D., Thantu, N., Melinger, J. S., Kim, S. K., and Lotshaw, W. T., 1996, *J. phys. Chem.*, **100**, 10389.
[36] Palese, S., Mukamel, S., Miller, R. J. D., and Lotshaw, W. T., 1996, *J. phys. Chem.*, **100**, 10380.
[37] Chang, Y. J., and Castner, E. W., Jr., 1993, *J. chem. Phys.*, **99**, 113.
[38] Chang, Y. J., and Castner, E. W., Jr., 1993, *J. chem. Phys.*, **99**, 7289.
[39] Chang, Y. J., and Castner, E. W., Jr., 1994, *J. phys. Chem.*, **98**, 9712.
[40] Castner, E. W., Jr., Chang, Y. J., Chu, Y. C., and Walrafen, G. E., 1995, *J. chem. Phys.*, **102**, 653.
[41] Chang, Y. J., and Castner, E. W., Jr., 1996, *J. phys. Chem.*, **100**, 3330.
[42] Quitevis, E. L., and Neelakandan, M., 1996, *J. phys. Chem.*, **100**, 10005.
[43] Neelakandan, M., Pant, D., and Quitevis, E. L., 1997, *Chem. Phys. Lett.*, **265**, 283.
[44] Neelakandan, M., Pant, D., and Quitevis, E. L., 1997, *J. phys. Chem.* A, **101**, 2936.
[45] Smith, N. A., Lin, S., Meech, S. R., and Yoshihara, K., 1997, *J. phys. Chem.* A, **101**, 3641.
[46] Shirota, H., Yoshihara, K., Smith, N. A., Lin, S., and Meech, S. R., 1997, *Chem. Phys. Lett.*, **281**, 27.
[47] Smith, N. A., and Meech, S. R., 2000, *J. phys. Chem.* A, **104**, 4223.
[48] Torre, R., Sánta, I., and Righini, R., 1993, *Chem. Phys. Lett.*, **212**, 90.
[49] Bartolini, P., Ricci, M., Torre, R., Sánta, I., and Righini, R., 1999, *J. chem. Phys.*, **110**, 8653.
[50] Idrissi, A., Ricci, M., Bartolini, P., and Righini, R., 1999, *J. chem. Phys.*, **111**, 4148.
[51] Cong, P., Deuel, H. P., and Simon, J. D., 1995, *Chem. Phys. Lett.*, **240**, 72.
[52] Wynne, K., Galli, C., and Hochstrasser, R. M., 1992, *Chem. Phys. Lett.*, **193**, 17.
[53] Steffen, T., Meinders, N. A. C. M., and Duppen, K., 1998, *J. phys. Chem.* A, **102**, 4213.
[54] Loughnane, B. J., Scodinu, A., Farrer, R. A., Fourkas, J. T., and Mohanty, U, 1999, *J. chem. Phys.*, **111**, 2686.
[55] Kamada, K., Ueda, M., Ohta, K., Wang, Y., Ushida, K., and Tominaga, Y., 1998, *J. chem. Phys.*, **109**, 10948.
[56] Winkler, K., Lindner, J., Bursing, H., and Vohringer, P., 2000, *J. chem. Phys.*, **113**, 4674.
[57] Berne, B. J., and Pecora, R., 1976, *Dynamic Light Scattering* (New York: Wiley).
[58] Steele, D., and Yarwood, J., 1991, *Spectroscopy and Relaxation of Molecular Liquids* (Amsterdam: Elsevier).
[59] Kivelson, D., and Madden, P. A., 1980, *Annu. Rev. phys. Chem.*, **31**, 523.
[60] Tabiscz, G. C., and Neumann, M. N., 1995, *Collision- and Interaction-Induced Spectroscopy* (Dordecht: Kluwer).

[61] Stassen, H., Dorfmüller, Th., and Ladanyi, B. M., 1994, *J. chem. Phys.*, **100**, 6318.
[62] Ladanyi, B. M., and Liang, Y. Q., 1995, *J. chem. Phys.*, **103**, 6325.
[63] Mukamel, S., 1995, *Principles of Nonlinear Optical Spectroscopy* (New York: Oxford University Press).
[64] Saito, S., and Ohmine, I., 1997, *J. chem. Phys.*, **106**, 4889.
[65] Ohmine, I., and Tanaka, H., 1990, *J. chem. Phys.*, **54**, 3846.
[66] Youngren, G. K., and Acrivos, K., 1975, *J. chem. Phys.*, **63**, 3846.
[67] Sension, R. J., and Hochstrasser, R. M., 1993, *J. chem. Phys.*, **98**, 2490.
[68] Hu, C.-M., and Zwanzig, R., 1974, *J. chem. Phys.*, **60**, 4354.
[69] Barklay, M. D., Kowalczyk, A. A., and Brand, L., 1981, *J. chem. Phys.*, **75**, 3581.
[70] Leggett, A. J., Chakravarty, S., Dorsey, A. T., Fisher, M. P. A., Garg, A., and Zwerger, W., 1987, *Rev. mod. Phys.*, **59,** 1.
[71] Bucaro, J. A., and Litovitz, T. A., 1971, *J. chem. Phys.*, **54**, 3846.
[72] Lotshaw, W. T., McMorrow, D., Dickson. T., and Kenney-Wallace, G. A., 1989, *Optics Lett.*, **14**, 309.
[73] Tanimura, Y., and Mukamel, S., 1993, *J. chem. Phys.*, **99**, 9496.
[74] Tanimura, Y., and Mukamel, S., 1994, in *Femtosecond Reaction Dynamics*, edited by D. A. Wiersma (Amsterdam: North-Holland), p. 157.
[75] Lynden-Bell, R. M., and Steele, W. A., 1984, *J. phys. Chem.*, **88**, 6514.
[76] Hesselink, W. H., and Wiersma, D. A., 1983, in *Spectroscopy and Excitation Dynamics of Condensed Molecular Systems*, edited by V. M. Agranovich, R. M. Hochstrasser (Amsterdam: North-Holland).
[77] Tominaga, K., and Yoshihara, K., 1995, *Phys. Rev. Lett.*, **74**, 3061.
[78] Tominaga, K., and Yoshihara, K., 1996, *J. chem. Phys.*, **104**, 4419.
[79] Steffen, T., and Duppen, K., 1996, *Phys. Rev. Lett.*, **76**, 1224.
[80] Steffen, T., and Duppen, K., 1997, *J. chem. Phys.*, **106**, 3854.
[81] Lin, S., Hands, I. D., Andrews, D. L., and Meech, S. R., 1999, *J. phys. Chem.* A, **103**, 3830.
[82] Hands, I. D., Lin, S., Meech, S. R., and Andrews, D. L., 2000, *Phys. Rev.* A, **62**, 23807.
[83] Blank, D. A., Kaufman, L. J., and Fleming, G. R., 1999, *J. chem. Phys.*, **111**, 3105.
[84] Kirkwood, J. C., Albrecht, A. C., and Ulness, D. J., 1999, *J. chem. Phys.*, **111**, 253.
[85] *Chem. Phys.*, **266** (2–3).
[86] Ladanyi, B. M., and Klein, S., 1996, *J. chem. Phys.*, **105**, 1552.
[87] Venturo, V. A., and Felker, P. M., 1993, *J. chem. Phys.*, **99**, 748.
[88] Zusman, L. D., 1980, *Chem. Phys.*, **49**, 295.
[89] Rips, I., and Jortner, J., 1987, *Chem. Phys. Lett.*, **133**, 411.
[90] Rips, I., and Jortner, J., 1987, *J. chem. Phys.*, **87**, 2090.
[91] Nagasawa, Y., Yartsev, A. P., Tominaga, K., Bisht, P. B., Johnstone, A. E., and Yoshihara, K., 1994, *J. chem. Phys.*, **101**, 5717.
[92] Yoshihara, K., Tominaga, K., and Nagasawa, Y., 1995, *Bull. Chem. Soc. Japan*, **68**, 696.
[93] Maroncelli, M., 1993, *J. molec. Liq.*, **57**, 1.
[94] Castner, Jr., E. W., Maroncelli, M., and Fleming, G. R., 1987, *J. chem. Phys.*, **86**, 1090.
[95] Maroncelli, M., MacInnis, J., and Fleming, G. R., 1989, *Science*, **243**, 1674.
[96] Maroncelli, M., 1991, *J. chem. Phys.*, **94**, 2084.
[97] Carter, E. A., and Hynes, J. T., 1991, *J. chem. Phys.*, **94**, 5961.
[98] Rosenthal, S. J., Xie, X., Du, M., and Fleming, G. R., 1991, *J. chem. Phys.*, **95**, 4715.
[99] Cho, M., Rosenthal, S. J., Scherer, N. F., Ziegler, L. D., and Fleming, G. R., 1992, *J. chem. Phys.* **96**, 5033.
[100] Maroncelli, M., Kumar, V. P., and Papazyan, A., 1993, *J. phys. Chem.*, **97**, 1.
[101] Smith, N. A., and Meech, S. R., 1997, *Faraday Discuss.*, **108**, 35.
[102] Smith, N. A., Meech, S. R., Rubtsov, I. V., and Yoshihara, K., 1999, *Chem. Phys. Lett.*, **303**, 209.

[103] Maroncelli, M., and Castner, E. W., Jr., 1998, *J. molec. Liq.*, **77**, 1.
[104] Raineri, F. O., and Friedman, H. L., 1994, *J. chem. Phys.*, **101**, 6111.
[105] Vöhringer, P., Arnett, D. C., Westervelt, R. A., Feldstein, M. J., and Scherer, N. F., 1995, *J. chem. Phys.*, **102**, 4027.
[106] Loughnane, B. J., and Fourkas, J. T., 1998, *J. phys. Chem.* B, **102**, 10288.
[107] Loughnane, B. J., Scodinu, A., and Fourkas, J. T., 1999, *J. phys. Chem.* B, **103**, 6061.
[108] Loughnane, B. J., Farrar, R. A., Scodinu, A., and Fourkas, J. T., 1999, *J. chem. Phys.*, **111**, 5116.
[109] Stankus, J. J., Torre, R., and Fayer, M. D., 1993, *J. phys. Chem.*, **97**, 9478.
[110] Deeg, F. W., Greenfield, S. R., Stankus, J. J., Newell, V. J., and Fayer, M. D., 1990, *J. chem. Phys.*, **93**, 3503.
[111] Torre, R., Rici, M., Saielli, G., Bartolini, P., and Righini, R., 1995, *Molec. Cryst. liq. Cryst.* A, **262**, 391.
[112] Lecalvez, A., Montant, S., Freysz, E., Ducasse, A., Zhuang, X. W., and Shen, Y. R., 1996, *Chem. Phys. Lett.*, **258**, 620.
[113] Shirota, H., and Castner, E. W., Jr., 2001, 10th International Conference on Time Resolved Vibrational Spectroscopy.
[114] Litvinenko, K., and Meech, S. R., unpublished.